Blood brain barrier precludes the cerebral arteries to intravenously-injected antisense oligonucleotide

Raphael Boursereau, Arnaud Donadieu, Fabrice Dabertrand, David Dubayle, Jean-Luc Morel

European Journal of Pharmacology 747 (2015) 141–149

Contents lists available at ScienceDirect

European Journal of Pharmacology

journal homepage: www.elsevier.com/locate/ejphar

Cardiovascular pharmacology

Blood brain barrier precludes the cerebral arteries to intravenously-injected antisense oligonucleotide

Raphael Boursereau [a,b,1], Arnaud Donadieu [a,b,1], Fabrice Dabertrand [c], David Dubayle [d], Jean-Luc Morel [a,b,*]

[a] Univ. de Bordeaux, Institut des Maladies Neurodégénératives, UMR 5293, F-33000 Bordeaux, France
[b] CNRS, Institut des Maladies Neurodégénératives, UMR 5293, F-33000 Bordeaux, France
[c] University of Vermont, Department of Pharmacology, UVM College of Medicine, Burlington, VT, USA
[d] Centre de Neurophysique, Physiologie, Pathologie, CNRS UMR 8119, Faculté des Sciences fondamentales et Biomédicales, Université Paris Descartes, 45, rue des Saints-Pères, 75006 Paris, France

ARTICLE INFO

Article history:
Received 19 August 2014
Received in revised form
20 November 2014
Accepted 24 November 2014
Available online 13 December 2014

Keywords:
Ryanodine receptor
Cerebral artery
Blood brain barrier
Calcium signaling

ABSTRACT

Alternative splicing of the ryanodine receptor subtype 3 (RyR3) produces a short isoform (RyR3S) able to negatively regulate the ryanodine receptor subtype 2 (RyR2), as shown in cultured smooth muscle cells from mice. The RyR2 subtype has a crucial role in the control of vascular reactivity via the fine tuning of Ca^{2+} signaling to regulate cerebral vascular tone. In this study, we have shown that the inhibition of RyR3S expression by a specific antisense oligonucleotide (asRyR3S) was able to increase the Ca^{2+} signals implicating RyR2 in cerebral arteries *ex vivo*. Moreover, we tried to inhibit the expression of RyR3S *in vivo*. The asRyR3S was complexed with JetPEI and injected intravenously coupled with several methods known to induce a blood brain barrier disruption. We tested solutions to induce osmotic choc (mannitol), inflammation (bacteria lipopolysaccharide and pertussis toxin), vasoconstriction or dilatation (sumatriptan, phenylephrine, histamine), CD73 activation (NECA) and lipid instability (Tween80). All tested technics failed to target asRyR3 in the cerebral arteries wall, whereas the molecule was included in hepatocytes or cardiomyocytes. Our results showed that the RyR3 alternative splicing could have a function in cerebral arteries *ex vivo*; however, the disruption of the blood brain barrier could not induce the internalization of antisense oligonucleotides in the cerebral arteries, in order to prove the function of RYR3 short isoform *in vivo*.

1. Introduction

The cerebrovascular network responds to the nervous system solicitations by modification of cerebral blood flow. The goal of this increase of functional hyperemia is to elevate the amount of glucose and oxygen. The vascular tone is due to vascular smooth muscle cells, and is in part encoded by Ca^{2+} signaling. The ryanodine receptors could be considered as the center of this signalisation. In fact, these Ca^{2+} channels, located in sarcoplasmic reticulum, encode several types of Ca^{2+} signals responsible for vasoconstriction (propagated Ca^{2+} waves), as well as vasodilatation (localized Ca^{2+} signals named Ca^{2+} sparks; for review Morel et al., 2007). As summarized in Fig. 1, ryanodine receptor subtypes (RyR1-3) are activated by an increase of intracellular Ca^{2+} concentration ($[Ca^{2+}]i$). This first increase of $[Ca^{2+}]i$ is due to Ca^{2+} entry and/or previous Ca^{2+} release from intracellular Ca^{2+} store. Thus, the ryanodine receptors encode the Ca^{2+}-induced Ca^{2+} release mechanism (CICR) to amplify Ca^{2+} waves necessary for vasoconstriction.

It is well established that RyR1 and RyR2 subtypes are implicated in Ca^{2+} waves, as well as Ca^{2+} sparks (Coussin et al., 2000). Various functions for RyR3 subtype were suggested. It could be implicated in spontaneous Ca^{2+} signals, as shown in cerebral arteries from RyR3 knockout mice (Löhn et al., 2001), as well as in the regulation of sarcoplasmic reticulum Ca^{2+} loading, as shown by antisense oligonucleotides strategy *ex vivo* (Mironneau et al., 2001). Finally, the alternative splicing of RyR3 generates complete long (RyR3L) and short (asRyR3S) isoforms in smooth muscle (Jiang et al., 2003). The RyR3S isoform can inhibit the RyR2 function, which increases the ryanodine receptor-dependent Ca^{2+} signaling (Jiang et al., 2003; Dabertrand et al., 2006). The RyR3L isoform is able to encode Ca^{2+} signals and thus participates

* Correspondence to: Institut des Maladies Neurodégénératives, UMR 5293 Université de Bordeaux/CNRS, 146 rue Leo Saignat, F-33000 Bordeaux, France. Tel.: +33 5 4000 8886.
E-mail addresses: Fabrice.Dabertrand@uvm.edu (F. Dabertrand), dubayle@biomedicale.univ-paris5.fr (D. Dubayle), jean-luc.morel@u-bordeaux.fr (J.-L. Morel).
[1] Equal participation in experimentations.

http://dx.doi.org/10.1016/j.ejphar.2014.11.027
0014-2999/

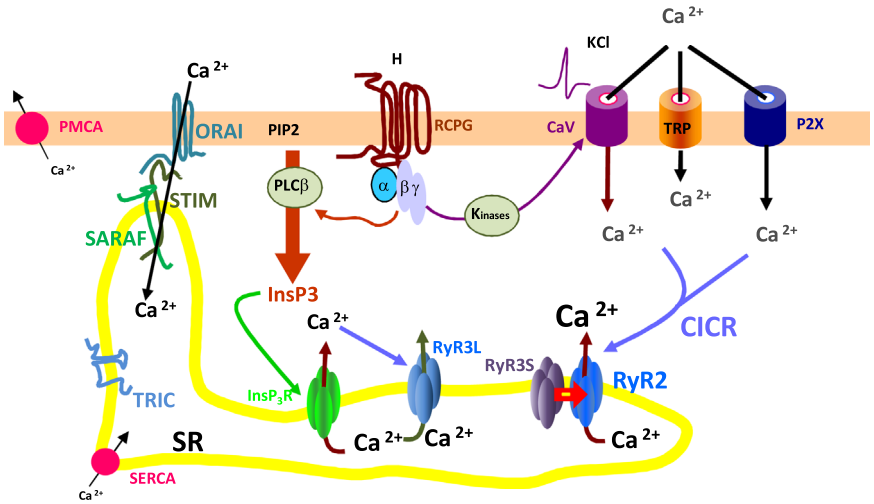

Fig. 1. Calcium signaling in vascular smooth muscle cells (VSMC). The Ca^{2+} entry (voltage-gated Ca^{2+} channels, ionotropic receptor as P2X, cationic channels as TRP) as well as InsP3-induced Ca^{2+} release are amplified by the CICR mechanism encoded by RyRs. Two different splice variant of RyR3 are co-expressed. The long isoform (RyR3L) is able to produce Ca^{2+} release whereas the short isoform (RyR3S) inhibits RyR2-dependent Ca^{2+} release. PMCA and SERCA encoded the extrusion of Ca^{2+} from cytoplasm to external compartment and sarcoplasmic reticulum (SR), respectively. FKBP12/12.6, sorcin were expressed and regulate RyR functions in vascular smooth muscle cell's Ca^{2+} signaling.

to the control of sarcoplasmic reticulum loading and modulation of spontaneous Ca^{2+} signaling (Dabertrand et al., 2008). Taken together, these data indicate that both isoforms of RyR3 are crucial for the regulation of Ca^{2+} signaling.

Firstly, all data concerning RyR3 isoforms were acquired in cultured cells (*ex vivo*) and their functions were never studied *in vivo*. Secondly, the fine regulation of Ca^{2+} signaling due to the splicing of RyR3 could participate in the regulation of functional hyperemia for the adaptation of the cerebral blood flow to neuronal activity.

Our goal was to study the RyR3 isoform functions *in vivo* by antisense oligonucleotide strategy to selectively decrease the expression of both isoforms in cerebral arteries in a mouse model.

Several techniques described below to address antisense oligonucleotide to cells into the cerebral artery wall were tested. Unfortunately, if the antisense oligonucleotide efficiency to inhibit RyR3 isoform was demonstrated in cerebral arteries in culture (*ex vivo*), the targeting of antisense oligonucleotide into cerebral arteries was not yet successful *in vivo*.

2. Materials and methods

2.1. Animals

The project was validated by the French ministry of research in accordance with European Community and French guiding principles. The principal investigator is authorized by French authorities to perform animal experiments (No C33-01-029). We have used 62 male C57BL/6J mice (Charles River, L'Arbresle, France). All animals were killed at the age of 4–6 months, by cervical dislocation or lethal injection of pentobarbital.

2.2. Treatments of mice to modulate the blood brain barrier (BBB) permeability

To induce the decrease of the expression of RyR3 splice variants *in vivo*, we injected intravenously a solution containing phosphorothioate antisense oligonucleotide (indicated with the prefix "as", for example asRYR3S targeted RYR3S isoform, asSCR is the scramble form of asRYR3 (Dabertrand et al., 2006)), coupled with JetPEI *in vivo* (Polyplus, Illkirsch, France) in a glucose solution (5%) following the recommendations of the supplier. Injections were performed via the retro-orbital way on anesthetized mice (Ketamine 1%, Xylazine 0.5% cocktail, 10 mL/Kg). The antisense oligonucleotide quantity was determined by the final volume unharmful for mice (200 μL, representing near 10% of blood volume).

We have also used the 2-O-methyl phosphorothioate oligoribonucleotide directed against exon 23 of the mouse dystrophin mRNA (asDYS) to test if the molecular structure is an important parameter.

Phosphorothioate antisense oligonucleotides were synthetized and coupled with Cy5 indomethacin at 5′ extremity (Eurogentec, Serain, Belgium). Therefore, cells containing antisense oligonucleotide were visualized by the fluorescence emitted at 680 nm.

The *in vivo* injection of antisense oligonucleotides was performed in association with a protocol inducing the temporary BBB disruption. The protocols were chosen and sometimes modified to be compatible with mouse survival during 4–5 days. Protocols are summarized in Table 1. Animals were killed by a lethal injection of pentobarbital.

Mannitol, pertussis toxin (PTx) (Sigma-Aldrich, St. Louis, MO) was diluted in 0.9% NaCl solution. NECA [1-(6-amino-9 *H*-purin-9-yl)-1-deoxy-*N*-ethyl-6-D-ribofuranuronamide], Tocris Biosciences, was dissolved in DMSO and before injection in 0.9% NaCl solution. Final concentration of DMSO was 0.5% (v/v).

2.3. Antisense oligonucleotide ex vivo

In this part of the study 25 mice were used. Cerebral arteries (anterior and middle cerebral artery trees) were discarded from brain, dissected and placed in vascular smooth muscle cell Lonza culture medium (Lonza, Levallois, France) containing antisense oligonucleotide (2×10^{-9} mol/well) and kept at 37 °C, 5% CO_2 during 2–4 days. Antisense oligonucleotides directed against RYR3 splice variants and RyR2 were previously described (Dabertrand et al., 2007; Dabertrand et al., 2008; Dabertrand et al., 2006). Phosphorothioate antisense oligonucleotides were synthetized and coupled with Cy3 indomethacin to visualize cells containing antisense oligonucleotide during Ca^{2+} measurement by the fluorescence at 568 nm. Animals were separated in several groups and treated as indicated in Table 2.

Table 1
Treatments applied to increase the permeability of the BBB.

Pharmacological agent	Dose	Effects	*n* (mice)	Reference
JetPEI efficiency			5	PolyPlus Protocol
Mannitol	2.6 g/kg 2 min before ASON i.v.	Osmotic choc	9	Rapoport (2000)
Lipopolysaccharide (LPS)	3 mg/kg 5 min before ASON i.v.	Inflammation	4	Xaio et al. (2001)
Pertussis toxin (PTx)	3.10^{-3} µg/µl 3 days before ASON i.v.	Inflammation	4	Clifford et al. (2007)
Sumatriptan	1 mg/kg 2 min before ASON i.v.	Vasoconstriction Blood pressure	4	Shepheard et al. (1995)
Phenylephrine	10 mg/kg 2 min before ASON i.v.	Vasoconstriction Blood pressure	6	Mueller and Heistad (1980), Mayhan (1996)
Histamine	30 mg/kg 2 min before ASON i.v.		4	
NECA	0.08 mg/kg 2 min before ASON i.v.	via CD73 activation	4	Carman et al. (2011), Mills et al. (2008)
Tween80		Lipid instability	4	

Table 2
Repartition of arteries and mice in all groups for *ex vivo* experiments.

Groups	Control	asSCR	asRyR3L	asRyR3S	asRyR3	asRyR2
Arteries (mice)	6 (4)	6 (5)	6 (4)	9 (5)	3 (3)	4 (4)

2.4. Cytosolic Ca^{2+} measurements

Arteries were prepared as previously described (Morel et al., 2014) to study the efficiency of antisense oligonucleotides to modulate Ca^{2+} signaling *ex vivo*. Briefly, arteries were placed on glass slides coated with CellTak™ (BD-Biosciences, Le-Pont-de-Claix, France) and loaded with 2×10^{-6} mol/L Fluo8-AM Ca^{2+} probe (Interchim, Montluçon, France), for 20 min at 37 °C in M199 culture medium (Life Technologies, Saint-Aubin, France). Slides were then mounted in the experimental chamber, perfused with physiological solution (NaCl 125 mM; KCl 5.6 mM; Hepes 8 mM; Glucose 11 mM; $MgCl_2$ 1 mM; $CaCl_2$ 2 mM; pH=7.45 at 20 °C). Imaging was performed with the confocal TCS SP5 system equipped with resonant scanner (Leica Microsystems, Nanterre, France) at 3.33 Hz in an image series mode.

To activate ryanodine receptors, applications of caffeine (Merck-Millipore, Nottigham, UK) were performed; to activate InsP3R, arteries were loaded with the membrane permeant derivative of caged InsP3: D-23-O-Isopropylidene-6-O-(2nitro-4,5-demethoxy) benzyl-myo-Inositol 1,4,5-trisphosphate-Hexakis (propionoxy-methyl)Ester (caged-145-InsP3; 2×10^{-6} mol/L; SiChem, Bremen, Germany) during 30 min before Fluo8-AM loading. Photolysis was produced by UV flash (10^{-3} s) from DIPSI (Chatillon, France).

2.5. Immunohistochemistry

To evaluate the efficiency of antisense oligonucleotide after Ca^{2+} measurements, the arteries were fixed by incubation in PBS solution containing 4% paraformaldehyde (15 min). The immunostaining was based on protocols previously described (Dabertrand et al., 2006). After fixation, vessels were washed 4 times and permeabilized in PBS containing 2% bovine serum albumin and 1 mg/ml saponin during 20 min and incubated overnight at 4 °C with the primary antibodies against RyR3 (anti-RyR3 Ab, AB9082, 1:100; Millipore, Billerica, MA) or against RyR2 (anti-RyR2 Ab, AB9080, 1:100; Millipore). The day after, cells were washed 4 times and incubated with the secondary Fluoprobe-488 antibody (Fluoprobes-Interchim Montluçon, France, 1:250) during 60 min at room temperature. After 3 washes in PBS, slides were mounted in Fluoromounted (Cliniscience, Nanterre, France). All parameters of SP5 confocal microscope were adjusted on non-specific labeled samples (arteries only incubated with secondary antibody) to maximally reduce the non-specific fluorescence. All parameters of SP5 confocal microscope were kept constant for all acquisitions to be compared. Means of pixel fluorescence were determined with each antisense oligonucleotide treatment and compared statistically to evaluate the decrease of protein expression.

2.6. RT-PCR

The protocol and primers were previously described (Dabertrand et al., 2006). The RNA was extracted with Masterpure RNA extraction kit (Epicenter); the reverse transcription reaction was performed on 50 ng RNA using the Sensiscript-RT kit (Qiagen) and PCRs were performed with hotstart Taq-polymerase (Qiagen) in a thermal cycler (Eppendorf). The annealing temperature was 60 °C. Relative amounts of amplicons were determined and normalized to the Glyceraldehyde-3-phosphate deshydrogenase (GAPDH).

2.7. Statistical analysis

Statistical analysis was performed with Prism software (Graphpad software Inc, La Jolla, CA). Data are expressed as means ± S.E.M.; *n* represents the number of tested cells or arteries. Significances between conditions were tested by one way ANOVA completed with a Tukey post-hoc test. p Values < 0.05 were considered as significant and indicated by★in figures.

3. Results

3.1. Efficiency of antisense oligonucleotide to inhibit RyR3 splice variants ex vivo

The expression of RyR3 splice variants and the efficiency of ASON were determined by RT-PCR (Fig. 2A). The quantification of

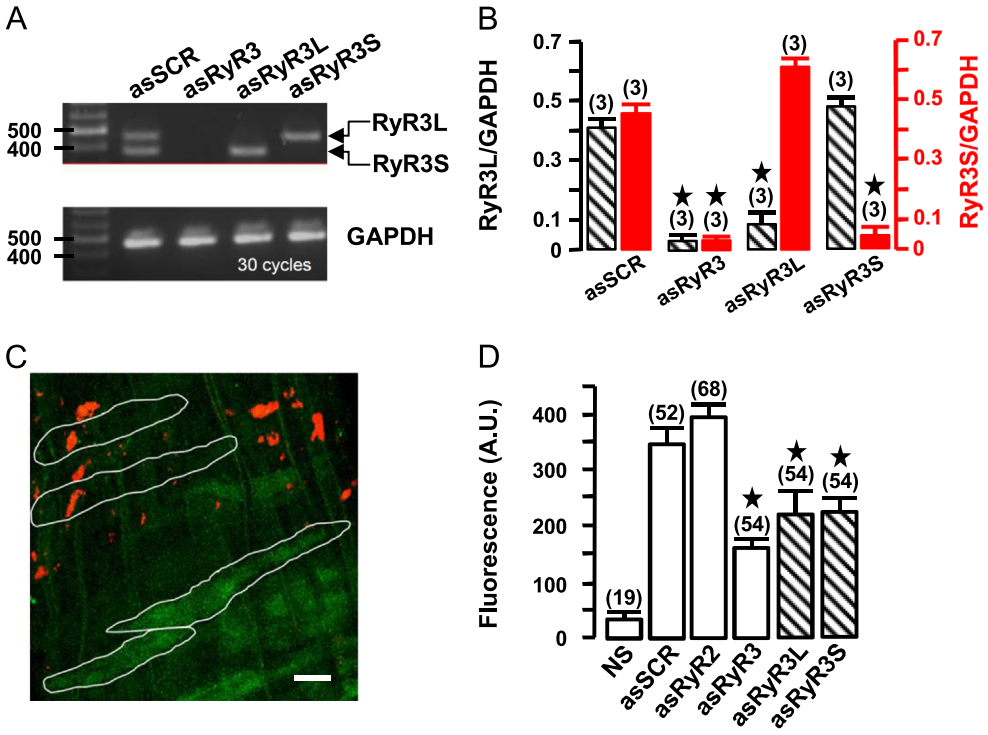

Fig. 2. Efficiency of ASON on expression of RyR3 splice variants. (A) Typical result of RT-PCR of RyR3 splice variants in arteries treated with antisense oligonucleotides. Fragments were stained with ethidium bromide and separated by electrophoresis in 2% agarose gel. (B) Means of relative expression of RyR3 splice variants in arteries treated with antisenses oligonucleotides (C) Typical immunostaining of RyR3 in CTL and asRyR3 treated arteries. Scale bar: 5 μm. (D) Intensity of immunostaining obtained with anti-RyR3 Ab (1/100) revealed with secondary anti-Rb-IgG coupled with FP488 (1/100). Data are expressed as means ± S.E.M.; (*n*) cells tested in 3–5 different experiments; ★$p < 0.05$.

RT-PCR via the calculation of the fluorescence ratios RyR3L/GAPDH and RyR3S/GAPDH indicated the efficiency of antisense oligonucleotides (Fig. 2B). To quantify the level of expression of RyR3 isoforms in vascular smooth muscle cells from whole cerebral arteries maintained in culture (*ex vivo*), the immunohistochemical labeling was performed with a specific anti-RyR3 antibody. As illustrated in Fig. 2C, the antisense oligonucleotide coupled to Cy5 was revealed not in all vascular smooth muscle cells. Only the level of fluorescence of cells containing ASON was measured 3 days after incubation in a culture medium containing antisense oligonucleotides. The asSCR as well as asRyR2 were not able to modify the expression of RyR3, whereas asRyR3 inhibited 50–60% of total immunostaining (Fig. 2D). Finally, the asRyR3L and asRYR3S significantly inhibited 25–30% of the fluorescence emitted by RyR3 immunolabelling (Fig. 2D). These results indicate that the expression of RyR3L and RyR3S could be reduced by the specific antisense oligonucleotide applied in *ex vivo* cultured arteries.

3.2. Inhibition of induced Ca^{2+} signals by antisense oligonucleotide ex vivo

The application of 10 mM caffeine induced the release of Ca^{2+} stored in sarcoplasmic reticulum by activation of ryanodine receptor in vascular smooth muscle cells incubated with all antisense oligonucleotide (Fig. 3A). As expected, the amplitudes of caffeine-induced Ca^{2+} signals were decreased in arteries incubated with asRyR2 and increased with asRyR3S (Fig. 3A–B). The ryanodine receptor was implicated in CICR to amplify Ca^{2+} entries and/or Ca^{2+} releases from Ca^{2+} stores (Fig. 1). To verify the potential physiological effects of antisense oligonucleotide, the Ca^{2+} signals evoked by depolarization and InsP3 were measured. The application of external solution containing 140 mM KCl depolarized the vascular smooth muscle cells and induced Ca^{2+} entry. The KCl-induced Ca^{2+} responses were increased in presence of asRyR3S and decreased in presence of RyR2 (Fig. 3C). After 30 min incubation with 10 μM ryanodine to block ryanodine receptor functions, the KCl-induced Ca^{2+} responses were similar in all conditions, indicating that antisense oligonucleotide treatment did not alter the Ca^{2+} entry. Interestingly, the Ca^{2+} responses induced by the photolysis of caged-InsP3 were similar in asSCR- and asRYR3S-treated cells, whereas in asRyR3L-treated cells the amplitude of InsP3-induced Ca^{2+} responses were significantly inhibited (Fig. 3D). These results indicate that RYR3S was not implicated in the amplification of Insp3-induced Ca^{2+} responses, whereas RyR3L could amplify this response.

Taken together, these results indicate that (1) the antisense oligonucleotides were able to be integrated within the vascular smooth muscle cells fromcerebral arteries in culture; (2) the antisense oligonucleotides were efficient *ex vivo* to modify the Ca^{2+} signaling; (3) RyR2 was responsible for the CICR and the RyR3S inhibited this mechanism; and (4) the RyR3L was probably implicated in the amplification of InsP3-induced Ca^{2+} responses.

3.3. Vascular smooth muscle cell integration of antisense oligonucleotide in vivo

To understand the physiological role of the alternative splicing of RyR3 in cerebral arteries, the antisense oligonucleotides directed against different RyR3 isoforms should be addressed *in vivo* specifically in vascular smooth muscle cells.

The carrier JetPEI was previously demonstrated to increase significantly the *in vivo* integration of antisense oligonucleotide via intraperitoneal (Dabertrand et al., 2012a) and intravenous pathways. When the asRyR3S associated with JetPEI was injected via intravenous pathway, various cell types were able to integrate the asRyR3, as for example hepatocytes (Fig. 4A). To be sure that JetPEI could also be efficient in the brain, the asRyR3S associated with JetPEI was injected directly into the cortex. All cells around the

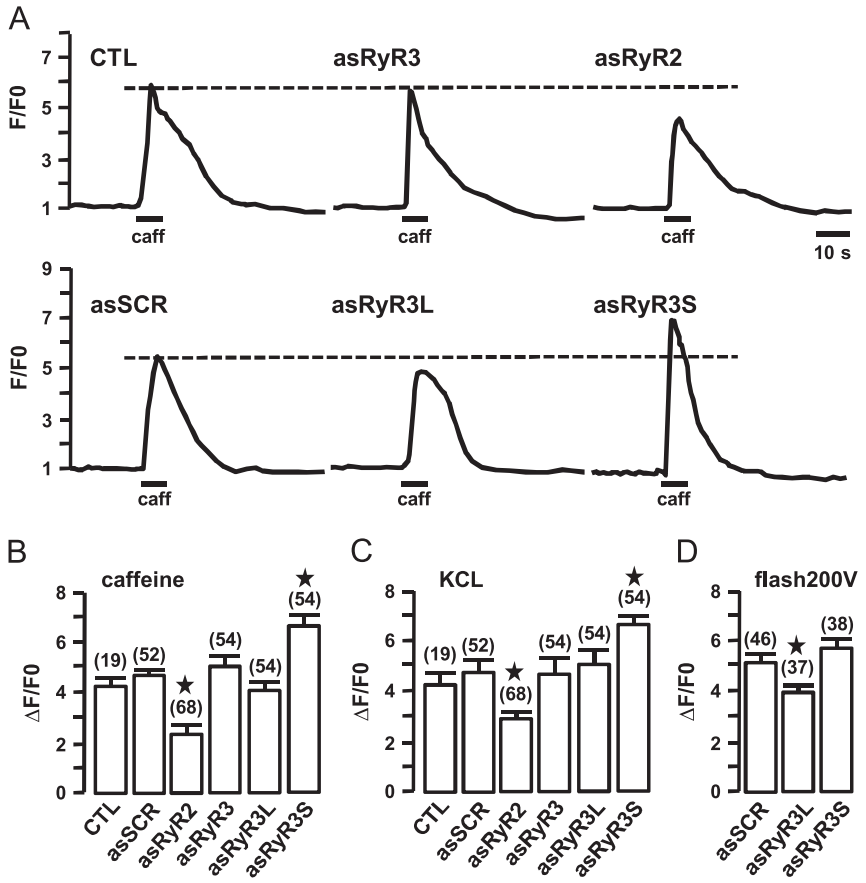

Fig. 3. Ex vivo efficiency of antisense oligonucleotides on caffeine and depolarization-induced calcium signals. (A) Typical calcium signal induced by caffeine application. (B) Mean of amplitude of calcium responses evoked by 10 mM caffeine. (C) Mean of amplitude of calcium responses evoked by 140 mM KCl. (D) Mean of amplitude of calcium responses evoked by photolysis (200 V) of caged-InsP3. Data are expressed as means ± S.E.M.; (*n*) cells tested in 3–5 different experiments; ★$p < 0.05$.

application site in brain parenchyma were potentially able to integrate antisense oligonucleotide (Fig. 4B–C). This result indicated that the intrathecal injection pathway to deliver antisense oligonucleotide was not specific. Thus, the intravenous pathway was tested to address antisense oligonucleotide only in vascular smooth muscle cells.

The intravenous injection of asRYR3S coupled to JetPEI alone was not able to target the wall of cerebral arteries (not shown); thus, the complex was injected in association with molecules able to induce a temporary disruption of BBB. Because our topic is to follow a potential effect of the modification of RyR3 isoform balance in cerebral arteries, we have used methods not deleterious for animal survival and cognitive functions. These methods are based on osmotic choc, neuroinflammation, drastic change in hemodynamics and membrane perturbations (Table 1). As illustrated in Fig. 5, all of these methods were not able to induce the integration of asRyR3S in wall cells of cerebral and intraparenchymal arteries. However, they were able to deliver the ASON in other cell types as hepatocytes. We found similar results with asSCR, asRyR3S, asRyR2 and asRyR3L, suggesting that the sequence of antisense oligonucleotides was not crucial for their integration into the vascular smooth muscle cells.

To verify that the antisense oligonucleotide coupled to JetPEI was able to pass through the vascular wall, we checked the crossing of molecules as dextran 150,000 coupled to FITC. Thirty minutes after the intravenous injection of dextran-FITC concomitantly with NECA, the presence of the dextran was revealed by confocal microscopy, as illustrated on the left of Fig. 6. The dextran was present at the periphery of the cerebral vessels, in the heart and also in the liver. We have obtained similar results with tween80 and phenylephrine (not shown). It is noticeable that the dextran labeling was much diffused and not present everywhere in the periphery of vessels. If some molecules passed through the wall vessels, the nature of the molecule could be important. That is why we compared the diffusion of asRyR3S and asDYS that we had previously used *in vivo* to target smooth muscle cells of portal vein and duodenum (Dabertrand et al., 2010; Morel et al., 2009). As illustrated in the center and the right of Fig. 6, the presence of asDYS was more important than the presence of asRyR3 in liver and heart, but in brain both asDYS and asRyR3S were not enough detected. Even after the BBB temporary disruption, the integration of asRyR3S was not possible via intravenous pathway.

4. Discussion

4.1. Function of RyR3 splice variants in cerebral arteries.

This study confirms that the alternative splicing of RyR3 is essential to the fine control of the Ca^{2+} signaling in smooth muscle cells. Indeed, the deletion of the RyR3S isoform increased the amplitude of Ca^{2+} signals in cerebral arteries as in duodenal and myometrium smooth muscle cells (Dabertrand et al., 2006, 2008). In cerebral arteries, RyR2 is central in the control of vascular tone via its ability to encode Ca^{2+} sparks (Dabertrand et al., 2012a; Jaggar et al., 1998; Sonkusare et al., 2012), but also Ca^{2+} waves responsible for vasoconstriction (Coussin et al., 2000; Morel et al., 1996). We confirmed in this model that Ca^{2+} waves

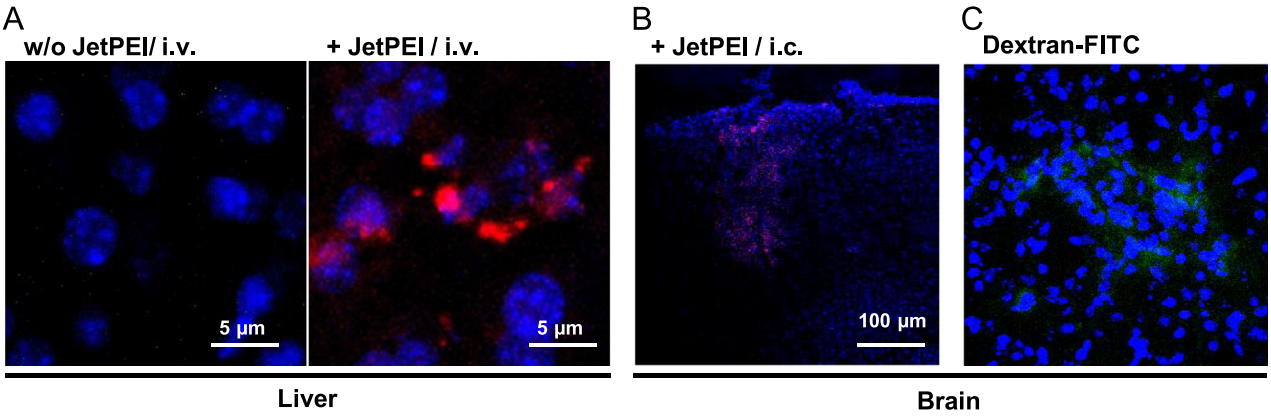

Fig. 4. Delivery of antisense oligonucleotides. (A) The association JetPEI increased the delivery of antisense oligonucleotides in liver cells. (B) Typical image after intra-cortical injection of antisense oligonucleotides-Cy5 in mouse brain. (C) Typical image of fluorescence of Dextran-FITC in brain parenchyma. Dextran appears in the proximity of intraparenchimal artery. Nucleuses are labeled with DAPI (blue) and antisense oligonucleotides-Cy5 is in red.

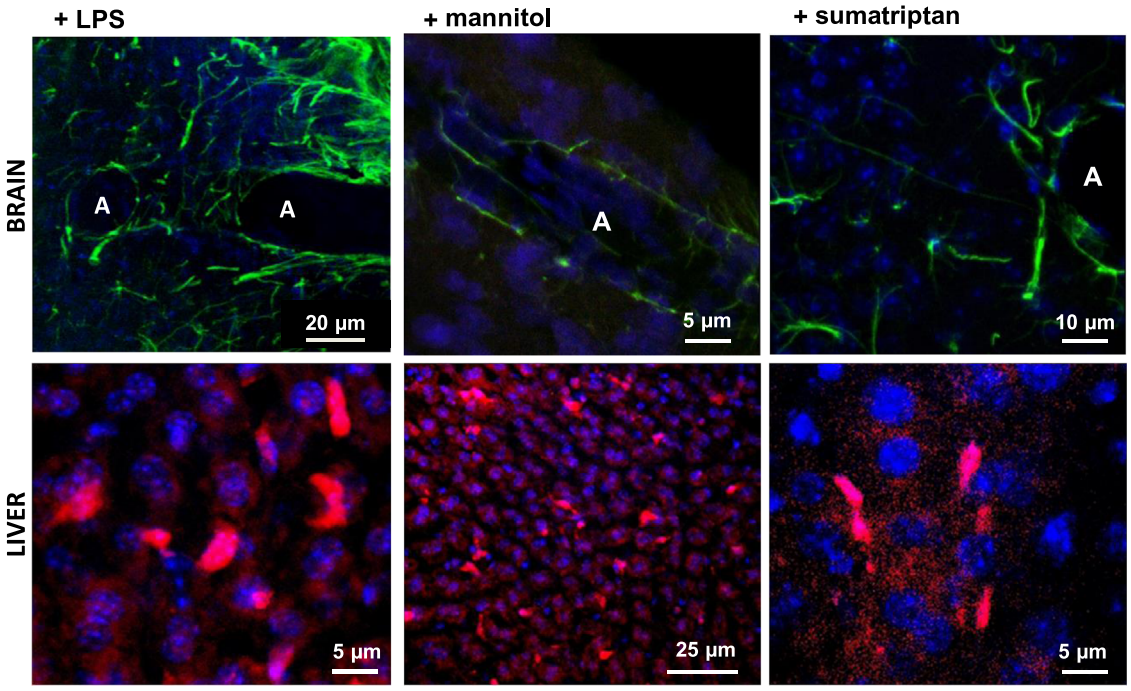

Fig. 5. Delivery of antisense oligonucleotides in brain (upper panel) and in liver (bottom panel). In brain slices, the astrocytes were labeled with GFAP antibody revealed by a secondary antibody coupled with fluoroprobe-488 and visualized in green. In both brain and liver the Cy5-asRyR3S was visualized in red and nucleuses of cells were stained with DAPI, in blue. The "A" indicates the lumen of cerebral arteries.

evoked by depolarization were modulated by RyR3S but not by RyR3L (Dabertrand et al., 2008, 2006).

Surprisingly, our results showed that RyR3L, but not RyR3S, could also participate to the Ca^{2+} signaling via the amplification of InsP3-dependent Ca^{2+} release. This last result could be due to the spatial repartition of ryanodine receptor and InsP3, as the spatial distribution of sarcoplasmic channels was determinant for Ca^{2+} signaling in smooth muscle (Gilbert et al., 2014). In cerebral arteries as in other vascular smooth muscle cells, the functional control of RyR3S on RYR2 could participate to the control of reactivity of cerebral arteries and that is why we tried to inhibit RyR3S expression in cerebral arteries *in vivo*.

4.2. Cellular intake antisense oligonucleotide

The inhibition of protein expression could be performed by several strategies using DNA or RNA molecules interacting with gene expressions. We have tested several strategies but only phosphorothioate antisense oligonucleotides selectively inhibited short or long splice variants of RyR3 (Dabertrand et al., 2006). The presence of antisense oligonucleotides in hepatocytes but not in the brain vessels indicated that it is possible to use them *in vivo*; however, the targeting in cerebral artery could be complicated. There are several explanations for these results including the delivery pathway, the nature of antisense oligonucleotide, and the targeted tissue.

The antisense oligonucleotides could be delivered either encoded in viral particles (Yasui et al., 2006) or coupled with molecules to encapsulate the DNA and then delivered by injections in blood stream (i.v.), in cavities, (i.p., i.c., …) or in tissues; alone and in association with technics to increase the accessibility to the targeted tissue (electroporation, sonication, …). The antisense oligonucleotide coupled with *in vivo* JetPEI could be addressed to several tissues as easily as demonstrated by the supplier and in this study in hepatocytes. We chose to inject it by i.v. because it was easier to use in classical animal facilities and could be used

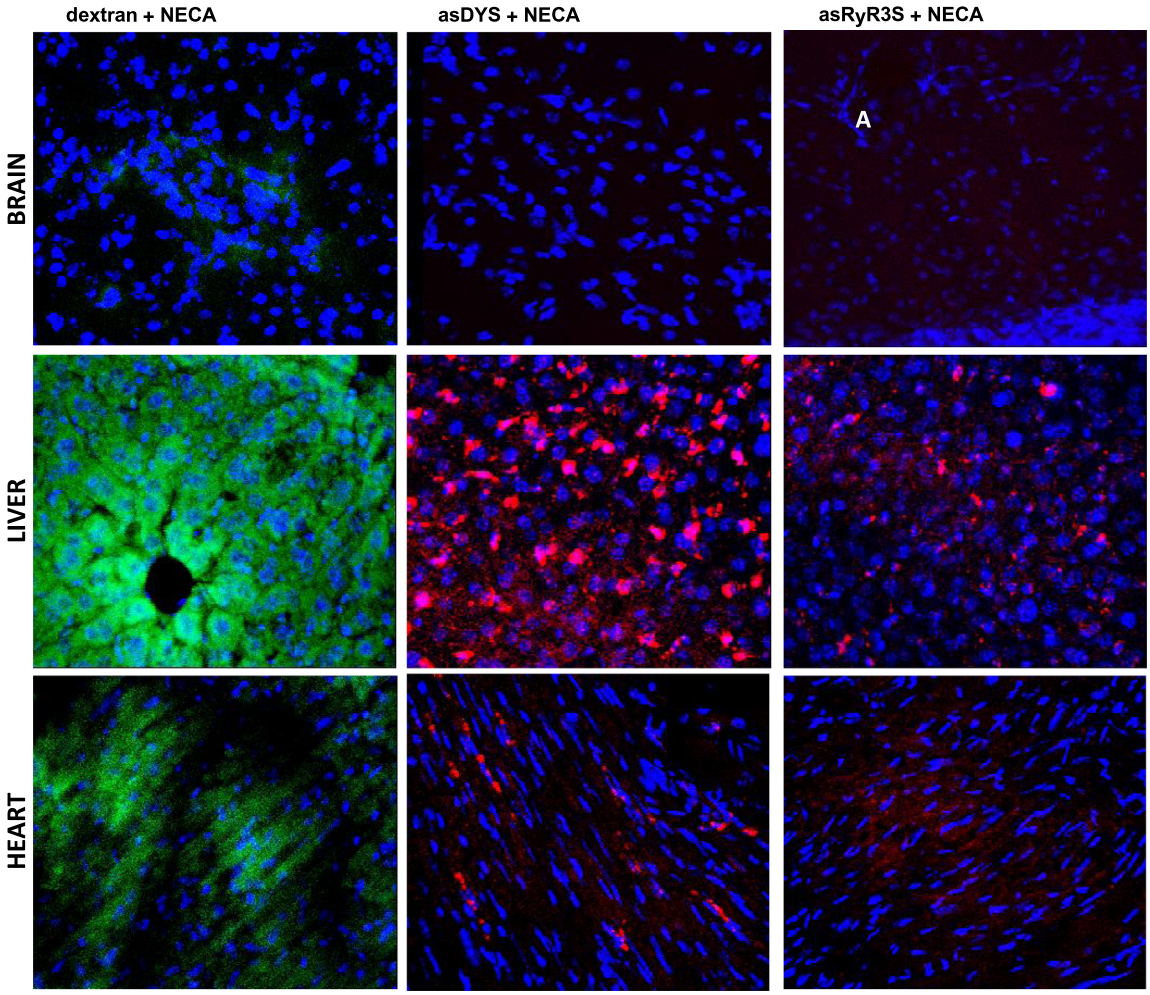

Fig. 6. Delivery of dextran-FITC, asDYS and asRyR3S in brain liver and heart. Dextran-FITC was in green; in both brain and liver the Cy5-asDYS and Cy5-asRyR3S were visualized in red and nucleus of cells were stained with DAPI, in blue.

ex vivo as well as *in vivo* to target smooth muscle cells or vessels (Dabertrand et al., 2010, 2012c; Park et al., 2012). We have excluded the intra-cerebroventricular pathway and brain electroporation (personnal data) because antisense oligonucleotides were detected in all cell types near the injection point and the distribution was restricted to a small area.

One hypothesis to explain the negative results to target, *in vivo*, cerebral arteries could be the decrease in the concentration of circulating antisense oligonucleotide via its elimination after binding to serum proteins and its limited absorption by vascular smooth muscle cells. If the monitoring of antisense oligonucleotides in blood extract could be verified, its presence in hepatocytes and in heart suggested that its bioavailability was not suppressed.

To increase the distribution of antisense oligonucleotide in the vessel wall, the blood brain barrier could be temporary disrupted by validated techniques (Table 1). The osmotic choc induced by mannitol was efficient to disrupt the BBB via intracarotid delivery (Liu et al., 2005; Rapoport, 2000; Rapoport et al., 1971). However, mainly the experiments previously reporting this technique indicated either that the mice were killed a few minutes or hours after surgery, or that it was used on bigger animals than mice. Finally, this method increases the risk of epileptic seizure (Marchi et al., 2007; Neuwelt et al., 2008). The injection pathway of mannitol is also determinant; in fact, similar doses of manitol injected in carotid and in venous pathways do not have similar effects on the BBB permeability (Chen et al., 2013). Our results showed that the increase of mannitol concentration did not modify the BBB permeability.

Moreover, the BBB disruption by inflammation processes should be controlled and induced with less deleterious agents than LPS and PTX or direct injection of histamine. Massive disruption of BBB produced by pathogenic agents induced the presence of the pathogen during days (Beghdadi et al., 2008).

NECA activating adenosine pathway (Carman et al., 2011) and phenylephrine could increase the passage of high weight molecules through the BBB [Légeron and Morel, ICCU2013: The CellViZio imaging system revealed the time course of BBB breakdown during phenylephrine-induced hypertension in the hippocampus of senescence accelerated mice (SAMP8)]. Our results suggested that: (1) the BBB disruption was not sufficient to induce the antisense oligonucleotide delivery in the cerebroarterial wall; and (2) the vascular cells were not able to integrate the antisense oligonucleotide coupled with JetPEI *in vivo*.

There is some evidence indicating that vascular smooth muscle cells can poorly integrate antisense oligonucleotide *in vivo*. Previously, we succeeded in delivering antisense oligonucleotide in hepatic portal vein, but the decrease in expression of the targeted protein was less than 30% (Dabertrand et al., 2012b; Morel et al., 2009). Nevertheless, antisense oligonucleotides were classically used *in vivo* (1) to modify the angiogenesis during neovascularization (Delvaeye et al., 2009; Hagigit et al., 2012; Park et al., 2012); (2) in order to limit pathological effects in vessels structurally modified, like after balloon injury (Hayashi et al., 2005) or vessel graft (Mann et al., 1995; Suzuki et al., 1997). Altogether, these studies indicated that in control conditions vascular smooth

muscle cells, especially in cerebral arteries, are not able to integrate antisense oligonucleotide with high efficiency.

The molecular nature of antisense oligonucleotide could also be implicated in bioavailability and cellular absorption. In fact, length, nucleotides' sequence and isoelectric point could be determinant for the *in vivo* efficiency of antisense oligonucleotide absorption (Prakash et al., 2001). For these reasons, we have tested the 2-O-methyl antisense ribonucleotide asDYS used in muscle, heart and smooth muscle cells to induce exon skipping in mdx mice (Partridge, 2010; Tanganyika-de Winter et al., 2012). The absorption by cardiomyocytes was better for asDYS than asRyR3S or RYR3L, but the cerebral arteries did not include asDYS. This suggested that cerebral arteries *in vivo* and in physiological conditions were not able to absorb antisense oligonucleotides with great efficiency.

5. Conclusions

These results are encouraging because they showed again that splicing variants could have a potential physiological role in *ex vivo* experiments; however, it remains to demonstrate *in vivo* functional reality. Our results showed that antisense oligonucleotide, coupled to a carrier, could not cross the BBB even if it could be maintained temporarily open. The major inconvenience of this situation is the difficulty to specifically address antisense oligonucleotide to cerebrovascular bed. In order to understand how Ca^{2+} signaling is involved in the regulation of functional hyperemia, it is thus very important to test other methods allowing the passage of antisense oligonucleotides in the vascular wall. These methods include coupling antisense oligonucleotides with peptides, grafting on nanoparticles or encapsulating. We must also find a way to increase the BBB permeability over a longer period by using physical methods such as the application of microwave fields.

Based on our results, it appears that it could be difficult to target vascular pathologies, after stroke for example, by antisense strategies. On the contrary, because the vessels irrigating the cerebral tumors are not similar to those of the BBB, antisense oligonucleotide could be used specifically as therapeutic drugs against tumor vessels, which are only constituted of endothelial cells, without tight junctions.

Finally, another advantage could be the use of antisense oligonucleotide vectorization techniques to target peripheral vascular pathologies without any effect on the central nervous system.

Acknowledgments

The authors thank Nathalie Biendon for technical assistance and Dr. Anne Prévot for reading of the MS. This work was supported by Grants from CNRS (AO longevite et vieillissement), CNES (DAR2013-5020) and Région Aquitaine (aging research grant 2009). RB, AD performed the experiments; FD, JLM and DD are responsible for experiment design, analysis of data and drafting the article. JLM was the Principal Investigator and has obtained the grants indicated here.

References

Beghdadi, W., Porcherie, A., Schneider, B.S., Dubayle, D., Peronet, R., Huerre, M., Watanabe, T., Ohtsu, H., Louis, J., Mecheri, S., 2008. Inhibition of histamine-mediated signaling confers significant protection against severe malaria in mouse models of disease. J. Exp. Med. 205, 395–408.

Carman, A.J., Mills, J.H., Krenz, A., Kim, D.G., Bynoe, M.S., 2011. Adenosine receptor signaling modulates permeability of the blood-brain barrier. J. Neurosci.: Off. J. Soc. Neurosci. 31, 13272–13280.

Chen, K.B., Wei, V.C., Yen, L.F., Poon, K.S., Liu, Y.C., Cheng, K.S., Chang, C.S., Lai, T.W., 2013. Intravenous mannitol does not increase blood–brain barrier permeability to inert dyes in the adult rat forebrain. NeuroReport 24, 303–307.

Clifford, P.M., Zarrabi, S., Siu, G., Kinsler, K.J., Kosciuk, M.C., Venkataraman, V., D'Andrea, M.R., Dinsmore, S., Nagele, R.G., 2007. Abeta peptides can enter the brain through a defective blood–brain barrier and bind selectively to neurons. Brain Res. 1142, 223–236.

Coussin, F., Macrez, N., Morel, J.L., Mironneau, J., 2000. Requirement of ryanodine receptor subtypes 1 and 2 for Ca(2+)-induced Ca(2+) release in vascular myocytes. J. Biol. Chem. 275, 9596–9603.

Dabertrand, F., Fritz, N., Mironneau, J., Macrez, N., Morel, J.L., 2007. Role of RYR3 splice variants in calcium signaling in mouse nonpregnant and pregnant myometrium. Am. J. Physiol. Cell Physiol. 293, C848–C854.

Dabertrand, F., Mironneau, J., Henaff, M., Macrez, N., Morel, J.L., 2010. Comparison between gentamycin and exon skipping treatments to restore ryanodine receptor subtype 2 functions in mdx mouse duodenum myocytes. Eur. J. Pharmacol. 628, 36–41.

Dabertrand, F., Mironneau, J., Macrez, N., Morel, J.L., 2008. Full length ryanodine receptor subtype 3 encodes spontaneous calcium oscillations in native duodenal smooth muscle cells. Cell Calcium 44, 180–189.

Dabertrand, F., Morel, J.L., Sorrentino, V., Mironneau, J., Mironneau, C., Macrez, N., 2006. Modulation of calcium signalling by dominant negative splice variant of ryanodine receptor subtype 3 in native smooth muscle cells. Cell Calcium 40, 11–21.

Dabertrand, F., Nelson, M.T., Brayden, J.E., 2012a. Ryanodine receptors, calcium signaling and regulation of vascular tone in the cerebral parenchymal microcirculation. Microcirculation.

Dabertrand, F., Porte, Y., Macrez, N., Morel, J.L., 2012b. Spaceflight regulates ryanodine receptor subtype 1 in portal vein myocytes in the opposite way of hypertension. J. Appl. Physiol. 112, 471–480.

Dabertrand, F., Porte, Y., Macrez, N., Morel, J.L., 2012c. Spaceflight regulates ryanodine receptor subtype 1 in portal vein myocytes in the opposite way of hypertension. J. Appl. Physiol. 1985 (112), 471–480.

Delvaeye, M., De Vriese, A., Zwerts, F., Betz, I., Moons, M., Autiero, M., Conway, E.M., 2009. Role of the 2 zebrafish survivin genes in vasculo-angiogenesis, neurogenesis, cardiogenesis and hematopoiesis. BMC Dev. Biol. 9, 25.

Gilbert, G., Ducret, T., Marthan, R., Savineau, J.P., Quignard, J.F., 2014. Stretch-induced Ca^{2+} signaling in vascular smooth muscle cells depend on Ca^{2+} store segregation. Cardiovasc. Res..

Hagigit, T., Abdulrazik, M., Valamanesh, F., Behar-Cohen, F., Benita, S., 2012. Ocular antisense oligonucleotide delivery by cationic nanoemulsion for improved treatment of ocular neovascularization: an in-vivo study in rats and mice. J. Controll. Release: Off. J. Controll. Release Soc. 160, 225–231.

Hayashi, K., Banno, H., Kadomatsu, K., Takei, Y., Komori, K., Muramatsu, T., 2005. Antisense oligodeoxyribonucleotide as to the growth factor midkine suppresses neointima formation induced by balloon injury. Am. J. Physiol. Heart Circ. Physiol. 288, H2203–H2209.

Jaggar, J.H., Wellman, G.C., Heppner, T.J., Porter, V.A., Perez, G.J., Gollasch, M., Kleppisch, T., Rubart, M., Stevenson, A.S., Lederer, W.J., Knot, H.J., Bonev, A.D., Nelson, M.T., 1998. Ca^{2+} channels, ryanodine receptors and Ca(2+)-activated K^+ channels: a functional unit for regulating arterial tone. Acta Physiol. Scand. 164, 577–587.

Jiang, D., Xiao, B., Li, X., Chen, S.R., 2003. Smooth muscle tissues express a major dominant negative splice variant of the type 3 Ca2+ release channel (ryanodine receptor). J.Biol.Chem. 278, 4763–4769.

Liu, R., Martuza, R.L., Rabkin, S.D., 2005. Intracarotid delivery of oncolytic HSV vector G47Delta to metastatic breast cancer in the brain. Gene Ther. 12, 647–654.

Löhn, M., Jessner, W., Fürstenau, M., Wellner, M., Sorrentino, V., Haller, H., Luft, F.C., Gollasch, M., 2001. Regulation of calcium sparks and spontaneous transient outward currents by RyR3 in arterial vascular smooth muscle cells. Circ. Res. 89, 1051–1057.

Mann, M.J., Gibbons, G.H., Kernoff, R.S., Diet, F.P., Tsao, P.S., Cooke, J.P., Kaneda, Y., Dzau, V.J., 1995. Genetic engineering of vein grafts resistant to atherosclerosis. Proc. Natl. Acad. Sci. USA 92, 4502–4506.

Marchi, N., Angelov, L., Masaryk, T., Fazio, V., Granata, T., Hernandez, N., Hallene, K., Diglaw, T., Franic, L., Najm, I., Janigro, D., 2007. Seizure-promoting effect of blood–brain barrier disruption. Epilepsia 48, 732–742.

Mayhan, W.G., 1996. Role of activation of bradykinin B2 receptors in disruption of the blood–brain barrier during acute hypertension. Brain Res. 738, 337–341.

Mills, J.H., Thompson, L.F., Mueller, C., Waickman, A.T., Jalkanen, S., Niemela, J., Airas, L., Bynoe, M.S., 2008. CD73 is required for efficient entry of lymphocytes into the central nervous system during experimental autoimmune encephalomyelitis. Proc. Natl. Acad. Sci. USA 105, 9325–9330.

Mironneau, J., Coussin, F., Morel, J.L., Barbot, C., Jeyakumar, L.H., Fleischer, S., Mironneau, C., 2001. Calcium signalling through nucleotide receptor P2X1 in rat portalvein myocytes. J. Physiol. 536, 339–350.

Morel, J.L., Fritz, N., Dabertrand, F., Macrez, N., 2007. Ca2+ releasing channels of smooth muscle sarcoplasmic reticulum. In: Savineau, J.P. (Ed.), New frontiers in smooth muscle biology and physiology. Transworld research network, Kerala, India, pp. 131–150.

Morel, J.L., Dabertrand, F., Fritz, N., Henaff, M., Mironneau, J., Macrez, N., 2009. The decrease of expression of ryanodine receptor sub-type 2 is reversed by gentamycin sulphate in vascular myocytes from mdx mice. J. Cell. Mol. Med. 13, 3122–3130.

Morel, J.L., Dabertrand, F., Porte, Y., Prevot, A., Macrez, N., Up-regulation of ryanodine receptor expression increases the calcium-induced calcium release and spontaneous calcium signals in cerebral arteries from hindlimb unloaded rats. Pflug. Arch.: Eur. J. Physiol. 466, 2014, 1517-1528.

Morel, J.L., Macrez-Lepretre, N., Mironneau, J., 1996. Angiotensin II-activated Ca^{2+} entry-induced release of Ca^{2+} from intracellular stores in rat portal vein myocytes. Br. J. Pharmacol. 118, 73–78.

Mueller, S.M., Heistad, D.D., 1980. Effect of chronic hypertension on the blood–brain barrier. Hypertension 2, 809–812.

Neuwelt, E., Abbott, N.J., Abrey, L., Banks, W.A., Blakley, B., Davis, T., Engelhardt, B., Grammas, P., Nedergaard, M., Nutt, J., Pardridge, W., Rosenberg, G.A., Smith, Q., Drewes, L.R., 2008. Strategies to advance translational research into brain barriers. Lancet Neurol. 7, 84–96.

Park, Y.S., David, A.E., Huang, Y., Park, J.B., He, H., Byun, Y., Yang, V.C., 2012. In vivo delivery of cell-permeable antisense hypoxia-inducible factor 1alpha oligonucleotide to adipose tissue reduces adiposity in obese mice. J. Controll. Release: Off. J. Controll. Release Soc. 161, 1–9.

Partridge, T., 2010. The potential of exon skipping for treatment for Duchenne muscular dystrophy. J. Child Neurol. 25, 1165–1170.

Prakash, T.P., Kawasaki, A.M., Johnston, J.F., Graham, M.J., Condon, T.P., Manoharan, M., 2001. Antisense properties of 2'-O-dimethylaminooxyethyl (2'-O-DMAOE) oligonucleotides. Nucleosides Nucleotides Nucleic Acids 20, 829–832.

Rapoport, S.I., 2000. Osmotic opening of the blood–brain barrier: principles, mechanism, and therapeutic applications. Cell. Mol. Neurobiol. 20, 217–230.

Rapoport, S.I., Hori, M., Klatzo, I., 1971. Reversible osmotic opening of the blood–brain barrier. Science 173, 1026–1028.

Shepheard, S.L., Williamson, D.J., Williams, J., Hill, R.G., Hargreaves, R.J., 1995. Comparison of the effects of sumatriptan and the NK1 antagonist CP-99,994 on plasma extravasation in Dura mater and c-fos mRNA expression in trigeminal nucleus caudalis of rats. Neuropharmacology 34, 255–261.

Sonkusare, S.K., Bonev, A.D., Ledoux, J., Liedtke, W., Kotlikoff, M.I., Heppner, T.J., Hill-Eubanks, D.C., Nelson, M.T., 2012. Elementary Ca^{2+} signals through endothelial TRPV4 channels regulate vascular function. Science 336, 597–601.

Suzuki, J., Isobe, M., Morishita, R., Aoki, M., Horie, S., Okubo, Y., Kaneda, Y., Sawa, Y., Matsuda, H., Ogihara, T., Sekiguchi, M., 1997. Prevention of graft coronary arteriosclerosis by antisense cdk2 kinase oligonucleotide. Nat. Med. 3, 900–903.

Tanganyika-de Winter, C.L., Heemskerk, H., Karnaoukh, T.G., van Putten, M., de Kimpe, S.J., van Deutekom, J., Aartsma-Rus, A., 2012. Long-term exon skipping studies with 2'-O-methyl phosphorothioate antisense oligonucleotides in dystrophic mouse models. Mol. Ther. Nucleic Acids 1, e44.

Xaio, H., Banks, W.A., Niehoff, M.L., Morley, J.E., 2001. Effect of LPS on the permeability of the blood–brain barrier to insulin. Brain Res. 896, 36–42.

Yasui, M., Yamamoto, H., Ngan, C.Y., Damdinsuren, B., Sugita, Y., Fukunaga, H., Gu, J., Maeda, M., Takemasa, I., Ikeda, M., Fujio, Y., Sekimoto, M., Matsuura, N., Weinstein, I.B., Monden, M., 2006. Antisense to cyclin D1 inhibits vascular endothelial growth factor-stimulated growth of vascular endothelial cells: implication of tumor vascularization. Clin. Cancer Res.: Off. J. Am. Assoc. Cancer Res. 12, 4720–4729.